

# Pointed Drawings of Planar Graphs

Oswin Aichholzer\*    Günter Rote†    André Schulz†  
Birgit Vogtenhuber\*

March 4, 2008

## Abstract

We study the problem how to draw a planar graph such that every vertex is incident to an angle greater than  $\pi$ . In general a straight-line embedding cannot guarantee this property. We present algorithms which construct such drawings with either tangent-continuous biarcs or quadratic Bézier curves (parabolic arcs), even if the positions of the vertices are predefined by a given plane straight-line embedding of the graph. Moreover, the graph can be embedded with circular arcs if the vertices can be placed arbitrarily. The topic is related to non-crossing drawings of multigraphs and vertex labeling.

## 1 Introduction

According to Fáry's theorem [5], every (simple) planar graph can be realized as plane straight-line embedding in the Euclidean plane. There is a vast literature dealing with the question of efficiently finding plane straight-line embeddings that fulfill certain (optimality) criteria. De Fraysseix, Pach and Pollack [4] and Schnyder [15] proved that every planar graph with  $n$  vertices can be drawn on a grid of size  $(n - 1) \times (n - 1)$ . The famous Koebe-Andreev-Thurston circle packing theorem [1, 7, 17] states that every planar graph can be embedded in a way such that its vertices correspond to interior disjoint disks, which touch if and only if the corresponding vertices are connected with an edge, see also [10, 2].

If we relax the condition that the given planar graph has to be simple, Fáry's theorem does not hold. The reason is that straight-line embeddings are not well defined for loops, or multiple edges between two vertices. However, one can ask how to draw planar multigraphs with loops crossing-free, where of course these

---

\*Institute for Software Technology, Graz University of Technology, [oaich|bvogt]@ist.tugraz.at, Supported by the Austrian FWF Joint Research Project 'Industrial Geometry' S9205-N12.

†Institut für Informatik, Freie Universität Berlin, Germany, [rote|schulza]@inf.fu-berlin.de

drawings require more complex edge shapes. Possible, but still rather simple candidates for such edges are polygonal chains, circular arcs, bi-arcs or splines.

A natural question is whether every planar multigraph can be drawn with circular arcs. Drawing multiple edges as circular arcs is no problem: an edge in a non-crossing straight-line drawing can be perturbed to any number of close-by circular arcs. Loops, however, require more space: The only circular arc between a vertex and itself is a full circle through this vertex; thus, an angle of  $\pi$  incident to this vertex must be free of other emanating arcs. (This angle is then sufficient for any number of parallel loops.) This naturally leads to the question of pointed drawings of simple graphs without loops. In a *pointed drawing* of a graph the incident edges of each vertex emanate within an open half plane.

Another potential application comes from drawing vertex labels. If the edges incident to a vertex point in all directions, it might be hard to place a label close to its vertex. Thus it is good to have some angular space without emanating edges.

Haas et al. [6] showed that a planar graph has a plane pointed drawing with straight-lines if and only if it is minimally rigid or a subgraph of a minimally rigid graph. A simple example of a graph that has no plane pointed embedding is the complete graph with four vertices.

Most recently, pointed drawings on the sphere have been studied by Gaiane Panina to construct virtual hyperbolic polytopes [12]. Drawings on the sphere can be used to describe the combinatorial structure of the normal cone of virtual polytopes. If such a drawing is furthermore pointed, the virtual polytope is hyperbolic. The construction of hyperbolic virtual polytopes disproved A.D Alexandrov's uniqueness conjecture for convex bodies [11].

**Definitions.** Throughout this paper, let  $G = (V, E)$  be a simple planar graph without loops, with finite vertex set  $V$  and finite set of edges  $E$ . In this paper we consider several types of plane embeddings  $\mathcal{F}(G)$ , all with some type of differentiable curves as edges.

For an embedding  $\mathcal{F}(G)$  we denote the embedding of a vertex  $v \in V$  by  $\mathcal{F}(v)$ , and the embedding of an edge  $e \in E$  by  $\mathcal{F}(e)$ . An embedding gives us a cyclic order of arcs leaving a vertex. The angle between two consecutive arcs is defined as the angle between the corresponding tangent rays.

For simplification, and as there is no risk of confusion, in the figures we will denote embedded vertices just by  $v$  instead of  $\mathcal{F}(v)$ .

**Definition 1 (Pointedness).** *A vertex in the embedding  $\mathcal{F}(G)$  is called pointed if it is incident to an angle greater than  $\pi$ . If all vertices of a drawing are pointed we call the drawing pointed.*

For the special case of straight-line embeddings, this definition is identical to the classic definition of pointedness, see [13, 14, 16].

**Variants of the Problem.** There are various incarnations of the problem how to draw a planar graph pointed. As mentioned before we can ask the

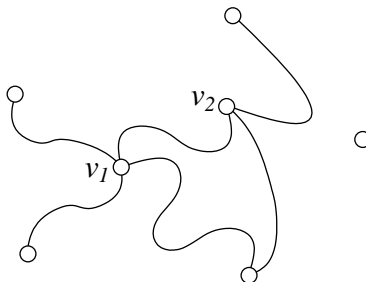


Figure 1: Embedding with a non-pointed vertex  $v_1$  and a pointed vertex  $v_2$ .

question for different kind of edge shapes. We study as *natural* edge shapes: circular arcs, tangent continuous biarcs and quadratic Bézier curves. Moreover the *quality of the pointedness* is an issue. For example, can we guarantee a free angular space around each vertex bigger than a given fixed angle larger than  $\pi$ ? For this stronger pointedness criterion we define the term  $\varepsilon$ -pointedness.

**Definition 2 ( $\varepsilon$ -Pointedness).** *Let  $\varepsilon > 0$  be a real number. A vertex in the embedding  $\mathcal{F}(G)$  is called  $\varepsilon$ -pointed if it is incident to an angle greater than  $2\pi - \varepsilon$ . We call a drawing  $\varepsilon$ -pointed if every vertex is  $\varepsilon$ -pointed.*

We can propose a stronger version of the pointed embedding problem. Given a planar straight-line embedding  $\mathcal{F}_s(G)$ . Can we draw a pointed drawing with a certain family of edge shapes *without* moving the points. We call an embedding with this property a *pointed redrawing*. The advantage of a pointed redrawing algorithm is clear, we can profit from the planar embedding and guarantee additional optimality criteria (i.e. place all vertices on a linear grid).

**Results.** In Section 2 we consider the problem of *pointed redrawings*. We show that every planar straight-line embedding  $\mathcal{F}_s(G)$  can be redrawn pointed and plane with Bézier curves as well as with tangent continuous biarcs. We also disprove that this is always possible by using circular arcs as edges.

Section 3 then deals with *pointed drawings* of (abstract) planar graphs. We prove that every planar graph can be drawn  $\varepsilon$ -pointed with Bézier curves, for arbitrary small epsilon. We show that by using biarcs as edges, every planar graph can be drawn such that for all vertices  $v$ , all incident edges share a common tangent at  $v$ . This is maybe one of the most beautiful results in this paper from an aesthetical point of view. Further we prove that every graph can be embedded pointed and plane with circular arcs as edges. For pointed embeddings with biarcs, Bézier curves or polygonal chains of length two, we give an explicit tight bound for the number of edges that cannot be drawn as straight-lines.

We summarize the results presented in this paper in Table 1. Note that essentially all obtained embeddings can easily be constructed.

edge shape	problem instance	answer
circular arcs	pointed drawing	possible, Theorem 3.3
	pointed redrawing	not possible, Theorem 2.3
tangent continuous	$\varepsilon$ -pointed drawing	possible, Theorem 3.2
biarcs	pointed redrawing	possible, Theorem 2.2
quadratic	$\varepsilon$ -pointed drawing	possible, Theorem 3.1
Bézier curves	pointed redrawing	possible, Theorem 2.1

Table 1: Results presented in this paper.

## 2 Pointed Redrawings

We start with the redrawing problem setting. Throughout this section we consider a plane straight-line embedding as input of our problem instance. Let this embedding be  $\mathcal{F}_s(G)$ .

**Theorem 2.1.** *There exists a pointed embedding  $\mathcal{F}_q(G)$  with quadratic Bézier curves as edges such that  $\mathcal{F}_q(v) = \mathcal{F}_s(v)$  for all  $v \in V$ . Moreover, for every  $v \in V$  the cyclic order of the edges incident to  $v$  in  $\mathcal{F}_s(G)$  is the same as in  $\mathcal{F}_q(G)$ .*

*Proof.* Without loss of generality assume that in  $\mathcal{F}_s(G)$  no two vertices have identical  $x$ -coordinates or  $y$ -coordinates. Assume further, that the vertices are sorted by  $y$ -coordinates in increasing order.

We construct the embedding  $\mathcal{F}_q(G)$  vertex by vertex from bottom to top. In each step we fix the embedding  $\mathcal{F}_q(e)$  of all edges  $e$  incident to the considered vertex  $v_i$ . Let  $h_i$  be the horizontal line through  $\mathcal{F}_s(v_i)$ . The basic idea is to redraw the edges incident to  $v_i$  such that they all emanate from  $\mathcal{F}_q(v_i)$  strictly on one side of  $h_i$  (which obviously guarantees pointedness). More precisely, for all but the first vertex we guarantee as an invariant that all drawn incident edges emanate below the according line  $h_i$ . As we never change an already drawn edge, every vertex remains pointed throughout the whole construction.

We start with adding the edges incident to  $v_1$  as straight-lines. Because  $\mathcal{F}_s(v_1)$  lies on the convex hull of  $\mathcal{F}_s(G)$ , by this  $\mathcal{F}_q(v_1)$  is pointed (and all edges are emanating from  $\mathcal{F}_q(v_1)$  above  $h_1$ ). Additionally, every edge  $\mathcal{F}_q(v_1v_j)$  emanates from  $\mathcal{F}_q(v_j)$  strictly below  $h_j$ .

When processing a vertex  $v_i, i \geq 2$ , all edges incident to a vertex  $v_j, j < i$ , have already been drawn (during the processing of  $v_j$ ). One can observe that these edges emanate from  $\mathcal{F}_q(v_i)$  strictly below the horizontal line  $h_i$  through  $\mathcal{F}_q(v_i)$ .

Let  $e_1, \dots, e_k$  be the edges incident to  $v_i$  that are not embedded yet and have positive slope in  $\mathcal{F}_s(G)$  (the edges “leaving”  $\mathcal{F}_s(v_i)$  towards up and right). Assume further that these edges are sorted by slope. Thus the edge  $e_1$  is the “rightmost edge” (the one with the smallest slope). We process these edges in increasing order. Let  $e = v_iv_l$  be the current edge we wish to add. Due to our

invariant we have the space to place a temporary point  $p_m$  below the line  $h_i$ , such that the triangle spanned by  $\mathcal{F}_q(v_i)$ ,  $p_m$  and  $\mathcal{F}_q(v_l)$  does not contain any vertex or part of an edge (see Figure 2). We use the triangle  $\mathcal{F}_q(v_i)p_m\mathcal{F}_q(v_l)$  as control polygon for a Bézier curve  $b$ . Since the convex hull of the control polygon is empty,  $b$  does not intersect any of the already embedded edges in  $\mathcal{F}_q(G)$ . Furthermore the line  $\mathcal{F}_q(v_i)p_m$  is a tangent of  $b$  at  $\mathcal{F}_q(v_i)$  and enters  $\mathcal{F}_q(v_i)$  from below. Likewise,  $p_m\mathcal{F}_q(v_l)$  is a tangent of  $b$  at  $\mathcal{F}_q(v_l)$  and enters  $\mathcal{F}_q(v_l)$  from below. Thus, by embedding the edge  $v_iv_l$  with  $b$ , the vertices  $v_i$  and  $v_l$  remain pointed in  $\mathcal{F}_q(G)$  and the invariant still holds.

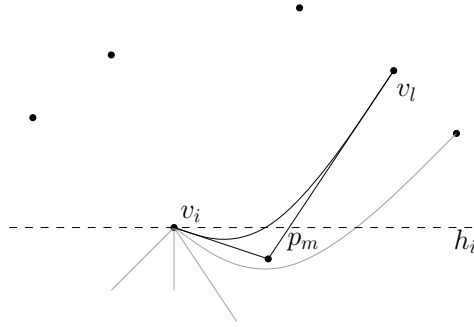


Figure 2: Construction of a plane pointed embedding where the edges are quadratic Bézier curves.

In this manner we embed all edges to the right of  $\mathcal{F}_q(v_i)$  and then apply a similar procedure for the edges emanating to the left of  $\mathcal{F}_q(v_i)$ . After processing all vertices in this way, we end with a pointed embedding  $\mathcal{F}_q(G)$ .  $\square$

The technique used in the proof of Theorem 2.1 can be modified to show a similar statement for (tangent continuous) biarcs due to the following observation.

**Lemma 2.1.** *Consider a triangle spanned by three points  $p_1, p_2$  and  $p_3$ . There exists a tangent continuous biarc connecting  $p_1$  with  $p_3$  that lies completely inside the triangle. Furthermore the biarc is tangent to  $p_1p_2$  at one end and tangent to  $p_3p_2$  at the other end.*

*Proof.* Assume that the segment  $p_1p_2$  is shorter than  $p_2p_3$ . We place a point  $\tilde{p}$  on the segment  $p_2p_3$  such that the length of  $p_2\tilde{p}$  is equal to the length of  $p_1p_2$ . (see Figure 3).

Let  $l_1$  be the line perpendicular to  $p_1p_2$  through  $p_1$  and let  $l_2$  be the line perpendicular to  $p_3p_2$  through  $\tilde{p}$ . The quadrilateral spanned by the intersection point of  $l_1$  and  $l_2$ ,  $p_1$ ,  $p_2$ , and  $\tilde{p}$  is a kite. Thus, there exists a circular arc passing through  $p_1$  and  $\tilde{p}$  with center  $l_1 \cap l_2$ . Since the angles of the kite at  $p_1$  and  $\tilde{p}$  equals  $\frac{\pi}{2}$ , the arc is tangent to  $p_1p_2$  at  $p_1$  and to  $p_2\tilde{p}$  at  $\tilde{p}$ . Let this arc be the first part of our biarc. The second part is given by the straight-line segment  $\tilde{p}p_3$  (a degenerate circular arc). The biarc is tangent continuous because the

circular arcs are tangent in the meeting point  $\tilde{p}$ . Thus, we are able to construct a biarc within the control polygon with the desired properties.  $\square$

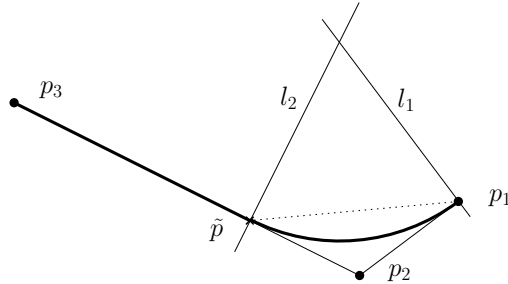


Figure 3: Embedding of an edge as a tangent continuous biarc in a triangle.

**Theorem 2.2.** *There exists a pointed embedding  $\mathcal{F}_b(G)$  with tangent continuous biarcs as edges such that  $\mathcal{F}_b(v) = \mathcal{F}_s(v)$  for all  $v \in V$ . Moreover, for every  $v \in V$  the cyclic order of the edges incident to  $v$  in  $\mathcal{F}_s(G)$  is the same as in  $\mathcal{F}_b(G)$ .*

*Proof.* We re-use the construction principle from the proof of Theorem 2.1. Of course, whenever we have chosen an appropriate empty triangle for an edge, instead of a Bézier curve, we place a tangent continuous biarc (from Lemma 2.1) inside it. Note that, because of the different type of curve, the triangles occurring throughout the construction will in general be different from the ones for the Bézier curves. Regardless of this, all arguments for correctness are still valid.  $\square$

We conclude this section with a negative result on pointed redrawings.

**Theorem 2.3.** *There exist planar graphs  $G = (V, E)$  with straight-line embeddings  $\mathcal{F}_s(G)$ , for which there are no pointed plane embeddings  $\mathcal{F}_c(G)$  with circular arcs as edges such that  $\mathcal{F}_c(v) = \mathcal{F}_s(v)$  for all  $v \in V$ .*

*Proof.* Consider the embedded plane straight-line star graph  $\mathcal{F}_s(G)$  shown in Figure 4(a), and let one of the tips of the star be  $v_t$ . This vertex is incident to the degree 5 vertex  $v_c$  in the center. In order to obtain a plane embedding  $\mathcal{F}_c(G)$ , any circular arc that is used to draw the edge  $v_t v_c$  has to pass through the narrow passage between  $\mathcal{F}_s(v_1)$  and  $\mathcal{F}_s(v_2)$ . Thus the possible space for embedding this edge is bounded by the intersection of the two (open) disks defined by the circumcircles of  $\mathcal{F}_s(v_t)\mathcal{F}_s(v_1)\mathcal{F}_s(v_c)$ , and  $\mathcal{F}_s(v_t)\mathcal{F}_s(v_2)\mathcal{F}_s(v_c)$  respectively (its boundary is drawn with dotted lines).

Because of the symmetry of  $\mathcal{F}_s(G)$ , the described situation occurs for each of the 5 edges incident to  $v_c$ . In order to make  $\mathcal{F}_c(v_c)$  pointed, we have to find valid embeddings (circular arcs) for two consecutive of such edges, such that their tangents at  $\mathcal{F}_c(v_c)$  span an angle larger than  $\pi$ . But the angle  $\alpha$  between the outer tangents of two neighbored regions is smaller than  $\pi$ , as can be seen from Figure 4(b). Thus, there is no way to obtain a plane embedding  $\mathcal{F}_c(G)$  where  $\mathcal{F}_c(v_c)$  is pointed.  $\square$

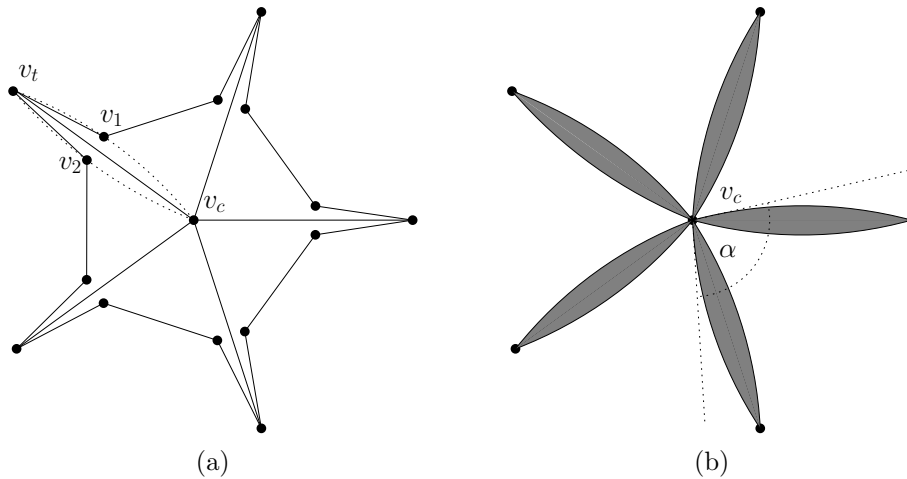


Figure 4: Star example of a plane embedding that can not be drawn pointed with circular arcs as edges.

Larger examples can be constructed easily. As long as a straight-line embedding similar to Figure 4(a) is contained inside another embedding, a pointed redrawing with circular arcs is impossible. Moreover, by adding more tips to the star, the largest possible angle free of emanating edges can be made arbitrary small.

### 3 Pointed Drawings

#### 3.1 Pointed Drawings with Bézier curves and Biarcs

In the last section we restricted ourselves to a predefined placement of the points, determined by a given plane straight-line embedding. If the location of the vertices can be chosen arbitrarily, we get the following easy consequence of Theorem 2.1.

**Theorem 3.1.** *For any  $\varepsilon > 0$  and any planar graph  $G$ , there exists an embedding  $\mathcal{F}_q(G)$  with quadratic Bézier curves where all vertices are  $\varepsilon$ -pointed.*

*Proof.* Consider an arbitrary straight-line embedding  $\mathcal{F}_s(G)$ . In the proof of Theorem 2.1 we showed a construction for a pointed embedding  $\mathcal{F}'_q(G)$ , in which all vertices point either to the bottom or to the top. Thus, by squeezing the embedding  $\mathcal{F}_s(G)$  in direction of the  $x$ -axis, the large angle on every vertex increases. This modification produces no crossings. Moreover, every transformed quadratic Bézier curve stays a quadratic Bézier curve (with respect to the squeezed control polygon).  $\square$

By similar arguments, it is possible to apply the construction in the proof of Theorem 2.1 in combination with Lemma 2.1 to an arbitrary straight-line embedding  $\mathcal{F}_s(G)$ , obtaining an  $\varepsilon$ -pointed embedding  $\mathcal{F}_b(G)$  with biarcs. However, in this case the argumentation is more involved, because squeezing a biarc does not result in a biarc. Thus, instead of deforming the already constructed embedding, we consider vertical double-wedges centered at every vertex, with wedge angle  $\varepsilon$ . We have to squeeze the original embedding in direction of the  $x$ -axis until all straight-line edges lie within these double-wedges. Further we have to modify our invariant. For all vertices, all embedded edges have now to emanate within one (upper or lower) half of the  $\varepsilon$ -double-wedge. By applying the original approach with the adopted invariant on the squeezed graph, we obtain an  $\varepsilon$ -pointed drawing with biarcs.

A disadvantage of these drawings (as well as of drawings obtained from the construction in the proof of Theorem 3.1) is the bad aspect ratio of its bounding box. For this reason, in the following we present a completely different approach for constructing a nicer pointed drawing with biarcs.

**Theorem 3.2.** *Every planar graph  $G = (V, E)$  has a pointed embedding  $\mathcal{F}_b(G)$  with tangent-continuous biarcs as edges such that  $\mathcal{F}_b(G)$  is  $\varepsilon$ -pointed for any  $\varepsilon > 0$ . Moreover, for every vertex  $v$  all edges incident to  $v$  share a common tangent at  $\mathcal{F}_b(v)$  in  $\mathcal{F}_b(G)$ . The directions of these tangents can be specified independently for each vertex.*

*Proof.* According to the Koebe-Andreev-Thurston circle packing theorem [1, 7, 17], there exists a straight-line embedding  $\mathcal{F}_s(G)$  such that the vertices of  $v \in V$  are embedded as the center points of disjoint disks. Moreover, two such disks touch if and only if the corresponding vertices are connected by an edge in  $G$ .

We start with such an embedding of the graph. To get our embedding  $\mathcal{F}_b(V)$  of the vertices by placing every vertex  $v \in V$  on an arbitrary point of the boundary of the disk corresponding to  $v$  in  $\mathcal{F}_s(G)$ , avoiding touching points of the disks.

Now consider an edge  $v_i v_j \in E$ . For the embedded vertex  $\mathcal{F}_b(v_i)$  let  $t_i$  be the tangent through  $\mathcal{F}_b(v_i)$  to its disk  $D_i$ . Furthermore, let  $p_{ij}$  be the touching point of the two adjacent disks  $D_i$  and  $D_j$  and let  $t_{ij}$  be the tangent to  $D_i$  and  $D_j$  through  $p_{ij}$  (see Figure 5). We draw a circular arc  $C_i$  from  $\mathcal{F}_b(v_i)$  to  $p_{ij}$  inside  $D_i$ , the center of  $C_i$  being the crossing of  $t_i$  and  $t_{ij}$ . Equivalently we draw an arc  $C_j$  from  $\mathcal{F}_b(v_j)$  to  $p_{ij}$  inside  $D_j$ , with center  $t_j \cap t_{ij}$ . We observe that both arcs meet in  $p_{ij}$  with the same tangent (orthogonal to  $t_{ij}$ ). Therefore the concatenation of  $C_i$  and  $C_j$  gives a tangent continuous biarc. We take  $C_i C_j$  as embedding for  $v_i v_j$  and apply this construction for all edges in  $E$ .

It is left to show that the constructed embedding is non-crossing. Clearly, a crossing of two biarcs could only appear within a disk of the circle packing. Consider all circular arcs emanating from the embedded vertex  $\mathcal{F}_b(v_i)$  as depicted in Figure 6. All corresponding circles have their centers on  $t_i$  and are passing through  $\mathcal{F}_b(v_i)$ , which lies on  $t_i$  too. Thus, all (and any two of) these circles intersect only in  $\mathcal{F}_b(v_i)$ , and the constructed embedding is plane.

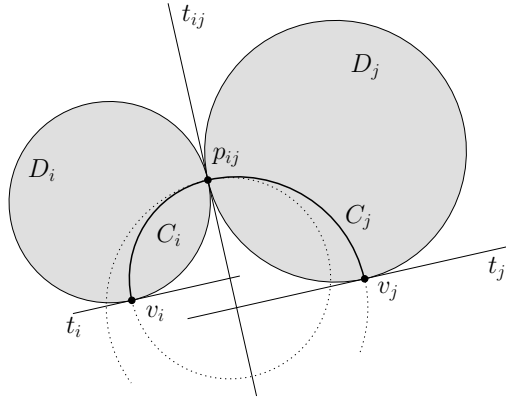


Figure 5: Construction of a tangent-continuous biarc from two touching disks  $D_i, D_j$ .

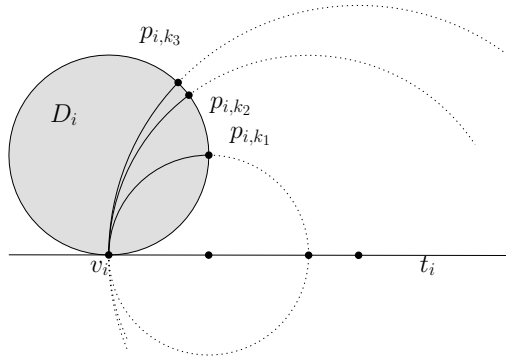


Figure 6: The situation at a vertex  $v_i$  that shows that the biarcs do not intersect.

All biarcs emanating from an embedded vertex  $\mathcal{F}_b(v_i)$  have a tangent orthogonal to  $t_i$ . We can determine this tangent by placing the vertex  $v_i$  on  $C_i$  appropriately.  $\square$

The above proof leaves some freedom to place the vertices on the boundaries of the related disks. If in the embedding  $\mathcal{F}_s(G)$  no two disk centers have the same  $x$ -coordinate, we can place each vertex on the bottommost point of the boundary of its disk. We then obtain a drawing where all vertices are pointed downwards, see Figure 7 for an example. By this, both arcs of the edges bend in the same direction. (There are no S-shaped biarcs.)

Another possibility is to place each vertex  $v_i \in V$  farthest away from any touching point of its disk  $D_i$ . In this way we can guarantee the radius of any circular arc inside  $D_i$  to be at least  $R_i \cdot \tan \frac{\pi}{2k_i}$ , where  $R_i$  is the radius of  $D_i$ , and  $k_i \geq 2$  is the degree of  $v_i$ .

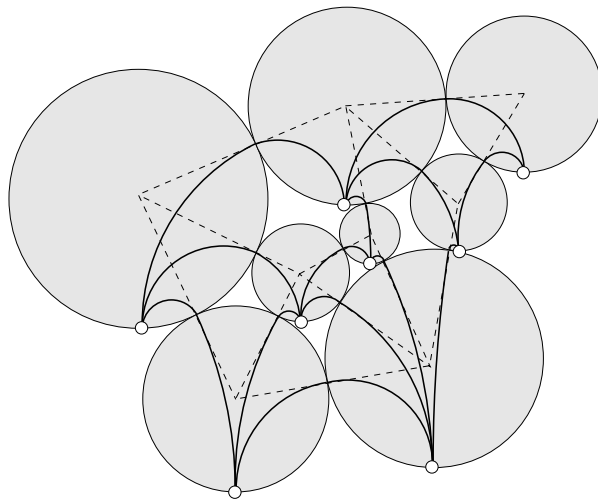


Figure 7: Pointed embedding with biarcs as edges, constructed from a circle packing.

### 3.2 Pointed Drawings with Circular Arcs

We continue with pointed drawings with circular arcs.

**Theorem 3.3.** *Every planar graph  $G$  has a pointed embedding with circular arcs as edges in which all vertices are pointed in the same direction.*

We prove the theorem by the following discussion. Let us assume that no two vertices in the embedding will get the same  $y$ -coordinate. Our drawing uses only special types of circular arcs and triangles:

**Definition 3 (upper horizontally tangent arc).** *Let  $p_1$  and  $p_2$  be two points, where  $p_1$  has the larger  $y$ -coordinate. We call a circular arc between  $p_1, p_2$  upper horizontally tangent (short *uht-arc*) if it passes through  $p_1$  and  $p_2$  and it has a horizontal tangent at  $p_1$ .*

**Definition 4 (upper horizontally tangent triangle).** *We call a drawing of a triangle upper horizontally tangent (short *uht-triangle*) if all of its edges are drawn as *uht-arcs*.*

Notice that for any two points the *uht-arc* is uniquely defined. Hence, for every point triple the *uht-triangle* is unique. We aim at constructing a drawing that contains *uht-triangles* only. We first introduce a drawing that will be “almost” pointed, this means that every vertex is incident to an angle equal or larger than  $\pi$ . In the following we restrict the straight-line edges to an absolute slope less or equal 1. This guarantees that the *uht-arcs* are  $x$ -monotone. We observe by the following lemmata that under certain assumption the *uht-triangles* behave nicely.

**Lemma 3.1.** Consider the uht-arc  $\mu$  between  $p_1$  and  $p_2$ . Let  $h_1$  be the horizontal line through  $p_1$ . Assume further that the absolute slope of  $p_1p_2$  is smaller than 1. Then the angle at  $p_1$  between  $h_1$  and  $\mu$  is twice as large as the angle at  $p_1$  between the  $p_1p_2$  and  $h_1$ .

*Proof.* The situation stated in the lemma is depicted in Figure 8. Let  $\alpha$  be the angle at  $p_1$  between  $h_1$  and  $p_1p_2$ . This angle is the alternate angle to the angle at  $p_2$  between  $h_2$  and  $p_2p_1$ . On the other hand,  $p_1p_2p_t$  is an isosceles triangle and hence the angle between  $p_1p_2$  and  $p_1p_t$  is  $\alpha$  as well. Thus, the angle between  $\mu$  and  $p_1p_2$  equals  $2\alpha$ .  $\square$

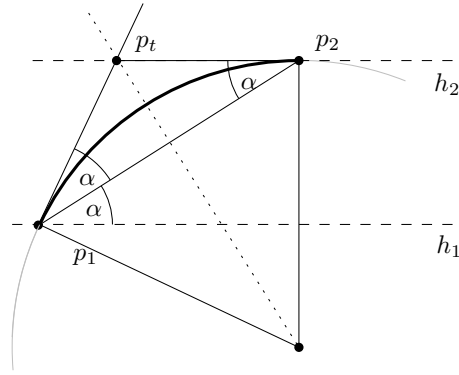


Figure 8: Construction used in the proof of Lemma 3.1.

**Lemma 3.2.** Consider three points  $p_1, p_2, p_3$  sorted by their  $x$ -coordinate. If

- (i) the absolute slope of the line segments  $p_1p_2, p_2p_3$  and  $p_1p_3$  is smaller than 1, and
- (ii)  $p_2$  lies below the line through  $p_1$  and  $p_3$ , or  $p_2$  has the highest  $y$ -coordinate, then

$p_1, p_2, p_3$  span a non-crossing uht-triangle that is oriented in the same way as the straight triangle  $p_1p_2p_3$ .

*Proof.* We prove the lemma by an easy case distinction. Let  $y_1, y_2, y_3$  be the  $y$ -coordinates of  $p_1, p_2, p_3$ . We denote with  $h_i$  the horizontal line passing through  $p_i$  and with  $a_{ij}$  the uht-arc between  $p_i$  and  $p_j$ . Without loss of generality we assume that  $y_1 < y_3$ . Depending on the relative location of  $y_2$  we obtain three cases. (see Figure 9).

**Case 1** ( $y_2 < y_1$ ):  $a_{13}$  and  $a_{23}$  cannot intersect since they touch at  $p_3$ . The other pairs of arcs have either disjoint ranges of  $x$ -coordinates or  $y$ -coordinates, and hence cannot intersect.

**Case 2** ( $y_1 < y_2 < y_3$ ): Again,  $a_{23}$  and  $a_{13}$  do not intersect since they touch at  $p_3$ . The arcs  $a_{12}$  and  $a_{23}$  are separated by the vertical line through  $p_2$  and

therefore do not intersect either. Since  $p_2$  lies below the line segment  $p_1p_3$ ,  $p_2$  must lie below the arc  $a_{13}$ . Due to Lemma 3.1 we know that the intersection between the tangent of  $a_{12}$  and  $h_1$  is twice as large as the intersection angle between  $p_1p_2$  and  $p_1p_3$ . It follows that  $a_{12}$  lies below  $a_{13}$  immediately to the right of  $p_1$ . Therefore,  $a_{12}$  and  $a_{13}$  cannot have another intersection (except  $p_1$ ), because otherwise, since  $a_{12}$  ends below  $a_{13}$ , they would have at least two additional intersection points, which is impossible. Thus, the orientation of the straight triangle coincides with the orientation of the associated uht-triangle.

**Case 3** ( $y_3 < y_2$ ): The uht-arcs  $a_{23}$  and  $a_{12}$  do not intersect since they are separated by a vertical line that passes through  $p_2$ . Similarly, the arcs  $a_{23}$  and  $a_{13}$  are separated by  $h_3$ . For the remaining pair of arcs  $a_{12}$  and  $a_{13}$  we apply again Lemma 3.1 and observe that  $a_{12}$  leaves  $p_1$  “above”  $a_{13}$ . Since  $a_{12}$  terminates above  $a_{13}$  (namely at  $p_2$ ), it follows similarly as in case 2 that  $a_{12}$  and  $a_{13}$  do not intersect.  $\square$

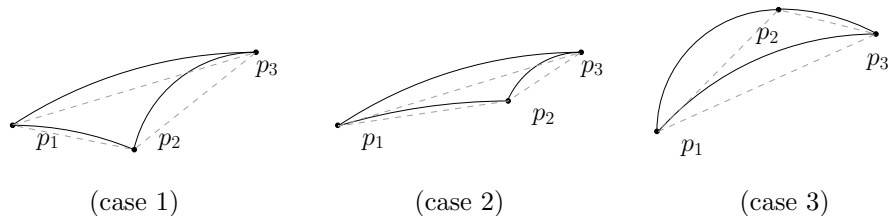


Figure 9: The three cases discussed in Lemma 3.2.

We continue by constructing a straight-line embedding that allows to substitute its triangles by uht-triangles. The basic idea goes back to the paper of De Fraysseix, Pach and Pollack [4].

**Theorem 3.4** ([4]). *A plane triangulated graph has a straight-line embedding on a  $(2n - 4) \times (n - 2)$  grid.*

By a slight extension of the inductive procedure which is used to prove Theorem 3.4 we can prove the following

**Theorem 3.5.** *A plane triangulated graph has a straight-line embedding on a  $(4n - 9) \times (2n - 4)$  grid, with the following additional properties:*

- (a) *No edge is vertical.*
- (b) *No edge is horizontal.*
- (c) *In each triangle face, the vertex with the middle x-coordinate is either the vertex with the highest y-coordinate, or it lies below the opposite edge.*

*Proof.* We first review the incremental construction of [4], see Figure 10. It inserts the vertices in a special (so-called canonical) order, such that the next

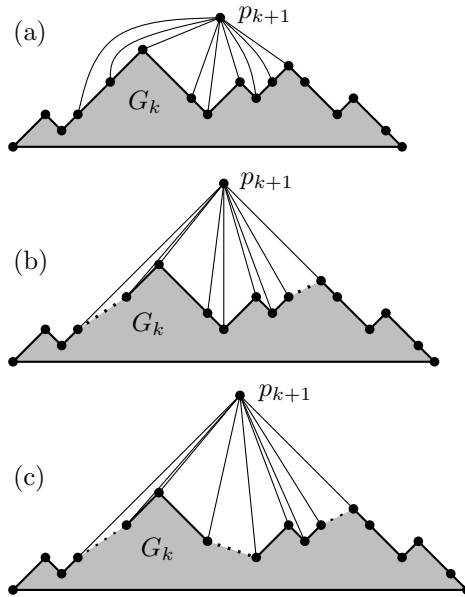


Figure 10: (a–b) The incremental step in the straight-line drawing algorithm of de Fraysseix, Pach and Pollack [4], and (c) the modification that prevents vertical edges.

vertex  $p_{k+1}$  that is inserted can be drawn on the outer face of the graph  $G_k$  induced by the first  $k$  vertices. Thereby we maintain as invariant that the outer boundary of the graph  $G_k$  (drawn so far) forms a chain of pieces of slope  $\pm 1$ , resting on a horizontal basis (Figure 10(a)). The next vertex  $p_{k+1}$  to be drawn is adjacent to a contiguous subsequence of vertices on the outer boundary. To make space for the new edges incident to  $p_{k+1}$ , the boundary of  $G_k$  is split into three pieces, which are separated from each other by shifting them one unit apart (Figure 10(b)). The middle piece contains all neighbors of  $p_{k+1}$  except the first and the last one. It can be shown that the whole graph  $G_k$  (inside the shaded area) can be shifted apart accordingly without creating crossings.

The newly created triangles always fulfill property (c), as can be checked directly, and no horizontal edges are created (property (b)). The only horizontal edge is the bottom base edge. This horizontal edge can easily be avoided by starting the construction with a non-horizontal base triangle in the first step.

To prevent vertical edges, one can split the middle part into two pieces and set them apart by two more units (Figure 10(c)). (*Two* units are necessary to ensure that the left and right part are separated in total by an even offset; this guarantees that the position of  $p_{k+1}$ , which is defined by the requirement that its leftmost and rightmost incident edges have slope  $+1$  and  $-1$  respectively, gets integer coordinates.) Thus, the dimensions of the grid increase by  $4 \times 2$  units for each new vertex. The initial drawing of the graph  $G_3$  with the first

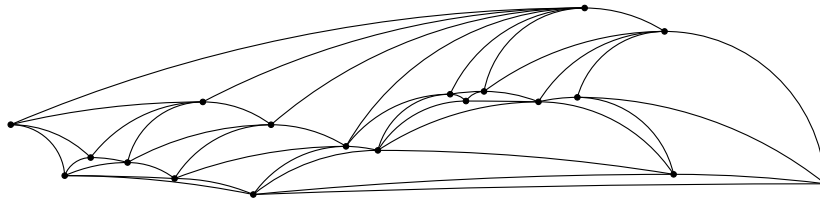


Figure 11: An example of a pointed drawing with circular arcs.

three vertices needs a  $3 \times 2$  grid. □

The slopes of the edges in the drawing are less than  $2n$ . By stretching the  $x$ -axis by a factor of  $2n$ , one obtains a drawing in which all edges have slopes in the range between  $-1$  and  $+1$ .

The straight-line embedding of Theorem 3.5 generates an embedding, which fulfills the conditions of Lemma 3.2. Therefore, we apply this embedding algorithm and substitute every straight triangle by the corresponding uht-triangle. We observe that around every vertex there is a number of edges that emanate in the horizontal direction, plus a number of additional edges that point upward. The latter type of edges have distinct tangent directions. Thus one can slightly bend every edge upward and achieve a pointed drawing with circular arcs.

Due to Theorem 3.5 the points of the embedding fit on a  $O(n) \times O(n^2)$  grid. An example of a pointed drawing with circular arcs that is constructed by our method is shown in Figure 11.

### 3.3 Pointed Drawings with Combinatorial Pseudo-Triangulations

A different way to find a pointed embedding utilizes the framework established in [6]. We can transform the abstract graph  $G$  into a so-called *combinatorial pseudo-triangulation* (defined in [9]) subdividing at most  $n - 3$  edges.

**Theorem 3.6.** *Every planar graph  $G$  with  $n$  vertices has a pointed embedding with either quadratic Bézier curves, biarcs, or polygonal chains consisting of two line segments, which uses at most  $n - 3$  non-straight edges. Moreover, for each inner vertex, one can arbitrarily choose a face in which it is pointed.*

*Proof.* We assume that the graph  $G$  is a triangulation (otherwise we add edges such that  $G$  becomes a triangulation and delete these edges after the embedding process). In the first step of the proof we construct a combinatorial pseudo-triangulation based on  $G$ . A combinatorial pseudo-triangulation is a combinatorial embedding of  $G$  with an assignment of the tags *large/small* to the angles of  $G$ . The outer face is determined as the face where every angle is large. Since  $G$  is a triangulation the combinatorial embedding is therefore uniquely (up to reflection). This defines the angles of  $G$  uniquely. The tag assignment to the angles has to guarantee three conditions: (1) The outer face contains only large

angles, (2) every vertex is incident to at most one large angle, and (3) every interior face contains exactly three small angles. Due to [6, Section 5.2] we can embed every combinatorial pseudo-triangulation such that every angle with *large* tag is larger than  $\pi$  in the embedding and every angle with *small* tag is smaller than  $\pi$  in the embedding. Furthermore, we can specify the affine shape of every face.

We construct the combinatorial pseudo-triangulation incrementally. In the beginning every angle of an interior face is gets the tag *small* (indicated by a small disk) and every angle at the outer face gets the tag *large* (indicated by a small circle). Clearly this assignment fulfills the three desired properties. Now we add the large interior angles on prescribed faces one by one. Changing a tag from *small* to *large* violates condition (3). This deficit can be repaired by subdividing an incident edge of the enlarged angle and give the new vertex the tags *small* (on the face where the deficit of small angles appears) and *large* (on the opposite face). This procedure is depicted in Figure 12. Now all three conditions hold and we continue.

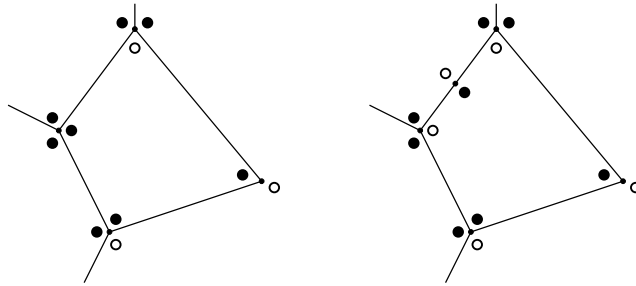


Figure 12: How to add a large angle tag (at the leftmost vertex) while maintaining a proper assignment of angle tags.

Notice that we add at most three large angle tags on every face. Thus we can assume that every edge is subdivided at most once. This can be achieved by subdividing always the edge that is left to the angle which gets the large angle tag with respect to some planar map.

We apply the embedding algorithm to realize the combinatorial pseudo-triangulation. Hereby, we prescribe the affine face shape such that it is guaranteed that in every interior face the vertices incident to a large angles can see each other, and every vertex incident to a large angle sees its opposite corner. Notice that the opposite corner is well-defined since all faces are pseudo-triangles. We depict the possible face shapes in Figure 13. Any affine transformation does not destroy the “visibility criteria” – otherwise the orientation of at a point triple reverses, which is only possible if we reverse all orientations.

What we have obtained so far is a pointed embedding, where at most  $n - 3$  edges are drawn as 2-chains (polygonal chains with 2 segments). We can substitute the 2-chains by Bézier curves or biarcs by the following construction:

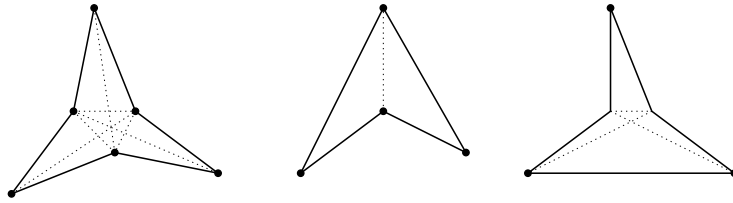


Figure 13: Affine shapes used for the embedding.

We complete every 2-chain to a triangle. This triangle is used as control polygon for the Bézier curves or the biarcs (see Lemma 2.1). Due to the affine shape of the faces the control polygons do not intersect. After inserting the arcs we remove the 2-chains and obtain the desired embedding.  $\square$

In general it is not possible to draw a pointed embedding with a larger number of straight-lines. In this sense, Theorem 3.6 is optimal. Let us remark that it is also possible to prove Theorem 3.6 without combinatorial pseudo-triangulations. This boils down to apply Tutte's spring embedding [18, 19] (the asymmetric case) for an augmented graph based on  $G$ . However, this approach would only reprove a special version of the embedding defined in [6].

Let us demonstrate the construction used in the proof of Theorem 3.6 by an example. Let  $G$  be the graph depicted in Figure 14(a). We want to obtain a pointed drawing where every interior vertex realizes the large angle at the central triangle. The appropriate combinatorial pseudo-triangulations (created with the methods of the proof of Theorem 3.6) is shown in Figure 14(b).

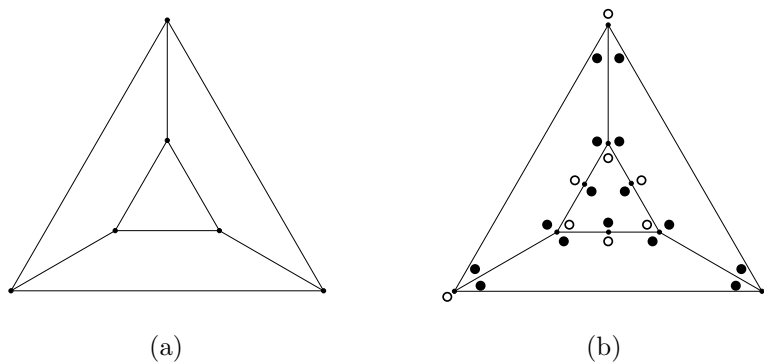


Figure 14: Construction of a combinatorial pseudo-triangulation as example.

We use the algorithm of [6] to embed the combinatorial pseudo-triangulation.

The result can be depicted in Figure 15(a). The 2-chains in the embedding can be completed to triangles. Using these triangles as control polygons for Bézier curves leads to Figure 15(b).

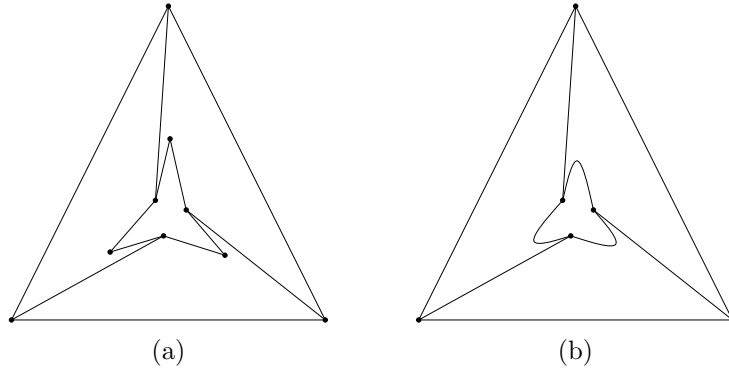


Figure 15: Pointed drawing with 2-chains (a) and biarcs (b) of the graph of Figure 14.

## 4 Conclusion

We have shown that every plane straight-line embedding can be redrawn pointed with identically embedded vertices, and either tangent-continuous biarcs or quadratic Bézier curves as edges. We can even ensure that all edges emanate from the vertices within an arbitrary small angle. These drawings are probably not satisfactory from an aesthetic point of view. Our embedding with biarcs, where all incident edges share a common tangent, is nicer and may be more useful for applications. Still, the construction we use relies on circle packings, which to compute is considered a hard problem, see for example [3, 8, 2] for algorithmic proofs. So it is an interesting question whether Theorem 3.2 can also be proven without using circle packings. Further, it remains open whether there exist aesthetically nice embeddings also for Bézier curves, or even for circular arcs.

The drawings with circular arcs that we construct (Theorem 3.3) result from perturbation and are just “barely” pointed, and edges emanate from a vertex almost in parallel directions. Also, the drawing fills a very oblong  $O(n^2) \times O(n)$  shape.

It remains open whether there are pointed embeddings with circular arcs (or with Bézier curves) that are aesthetically more pleasing.

**Acknowledgments.** Research on this topic was initiated during the fourth European Pseudo-Triangulation Week in Eindhoven (the Netherlands), organized by Bettina Speckmann. We would like to thank Thomas Hackl, Michael

Hoffmann, David Orden, Michel Pocchiola, Jack Snoeyink, and Bettina Speckmann for the inspiring spirit and for many valuable discussions.

## References

- [1] E. M. Andreev. On convex polyhedra in Lobacevskii space. *Math. USSR Sbornik*, 10(3):413–440, 1970.
- [2] Y. Colin de Verdière. Un principe variationnel pour les empilements de cercles. *Invent. Math.*, 104(3):655–669, 1991.
- [3] C. R. Collins and K. Stephenson. A circle packing algorithm. *Comput. Geom. Theory Appl.*, 25(3):233–256, 2003.
- [4] H. de Fraysseix, J. Pach, and R. Pollack. How to draw a planar graph on a grid. *Combinatorica*, 10(1):41–51, 1990.
- [5] I. Fáry. On straight line representations of planar graphs. *Acta Univ. Szeged. Sect. Sci. Math.*, 11:229–233, 1948.
- [6] R. Haas, D. Orden, G. Rote, F. Santos, B. Servatius, H. Servatius, D. Souvaine, I. Streinu, and W. Whiteley. Planar minimally rigid graphs and pseudo-triangulations. *Computational Geometry, Theory and Applications*, 2005.
- [7] P. Koebe. Kontaktprobleme der konformen Abbildung. *Ber. Verh. Sächs. Akademie der Wissenschaften Leipzig, Math.-Phys. Klasse*, 88:141–164, 1936.
- [8] B. Mohar. A polynomial time circle packing algorithm. *Discrete Math.*, 117(1-3):257–263, 1993.
- [9] D. Orden, F. Santos, B. Servatius, and H. Servatius. Combinatorial pseudo-triangulations. *Discrete Mathematics*, 307(3-5):554–566, 2007.
- [10] J. Pach and P. K. Agarwal. *Combinatorial geometry*. Wiley-Interscience Series in Discrete Mathematics and Optimization. John Wiley & Sons Inc., New York, 1995. A Wiley-Interscience Publication.
- [11] G. Panina. New counterexamples to A. D. Alexandrov’s hypothesis. *Adv. Geom.*, 5(2):301–317, 2005.
- [12] G. Panina. On hyperbolic virtual polytopes and hyperbolic fans. *Central European Journal of Mathematics*, 4(2):270–293, 2006.
- [13] M. Pocchiola and G. Vegter. Pseudo-triangulations: theory and applications. In *SCG ’96: Proceedings of the twelfth annual symposium on Computational geometry*, pages 291–300, New York, NY, USA, 1996. ACM.

- [14] M. Pocchiola and G. Vegter. The visibility complex. *Internat. J. Comput. Geom. Appl.*, 6(3):279–308, 1996. ACM Symposium on Computational Geometry (San Diego, CA, 1993).
- [15] W. Schnyder. Embedding planar graphs on the grid. In *SODA '90: Proceedings of the first annual ACM-SIAM symposium on Discrete algorithms*, pages 138–148, Philadelphia, PA, USA, 1990. Society for Industrial and Applied Mathematics.
- [16] I. Streinu. A combinatorial approach to planar non-colliding robot arm motion planning. In *41st Annual Symposium on Foundations of Computer Science (Redondo Beach, CA, 2000)*, pages 443–453. IEEE Comput. Soc. Press, Los Alamitos, CA, 2000.
- [17] W. P. Thurston. The geometry and topology of 3-manifolds. Note, Princeton University, 1988.
- [18] W. T. Tutte. Convex representations of graphs. *Proceedings London Mathematical Society*, 10(38):304–320, 1960.
- [19] W. T. Tutte. How to draw a graph. *Proceedings London Mathematical Society*, 13(52):743–768, 1963.